DOI: 10.1002/chem.200901693

On the Coherent Description of Diffusion-Influenced Fluorescence Quenching Experiments II: Early Events

Gonzalo Angulo,*[a] Daniel R. Kattnig,[b] Arnulf Rosspeintner,[b] Günter Grampp,[b] and Eric Vauthey[c]

Abstract: In a previous article we showed how to perform and analyze steady-state and nanosecond time-resolved experiments on fluorescence quenching by electron transfer in a coherent manner. Now, by making use of a superior time resolution, we explore the first stages of this kind of reaction. The novel information gained enables us to merge the results on the viscosity and the driving-force dependencies of the reaction rate. A unique set of parameters for a single reaction channel suffices to describe all the results in the frame of differential encounter theory for diffusion-influenced, bimolecular, remote electron-transfer reactions. The inclusion of the solvent structure is crucial for the understanding of the reaction kinetics. To the authors' best knowledge, this is the first time that such a comprehensive set of data has been successfully and jointly explained in the field, with physically sound parameters for electron-transfer reactions.

Keywords: diffusion · differential encounter theory · electron transfer · fluorescence · quenching

Introduction

Electron transfer is one of the simplest and most important chemical reactions. Triggering the reaction by light reveals detailed information on the reaction dynamics down to the femtosecond timescale. This implies that photoinduced electron-transfer reactions can be studied on the same timescale as that of vibrational motion. For bimolecular reactions, the Brownian motion of freely diffusing species in liquid solution strongly affects the observed kinetics.[1] Therefore, freezing the relative motion of the reaction partners by chemical linking[2–4] or by studying the reaction in rigid media[5,6] have been common strategies to overcome the unmitigated electron-transfer events. Unfortunately, these approaches either modify the reactants or the reaction medium. In order to study the behavior of the bimolecular reaction directly in liquid media, the use of very short (with respect to the timescale of translational diffusion) laser pulses is compulsory. For example, the excited-state dynamics can be monitored by means of the fluorescence decay of one of the reactants, which is a very sensitive technique. Thus, the diffusion at very short times should not mask the dynamics of the reaction that proceeds during the so-called static quenching regime of fluorescence. So far, several attempts have been made with this aim.[7–13] The valuable results obtained are often difficult or even impossible to compare with the quenching experiments performed on the nanosecond timescale,[7] or additional reaction channels have to be invoked,[12,13] or the electron-transfer parameters obtained from the experiments are beyond the range of applicability of the diabatic electron-transfer model employed.[8,9,12–18] Especially troublesome is the task of merging the reaction kinetics obtained on different timescales and under different conditions: it has been puzzling to compare the ultrafast techniques with slower ones, as well as with the steady-state measurements (or time-integrated kinetics). Furthermore, the dependence of the kinetics on the medium properties or on the driving force of the reaction has also been a matter of discussion.[19]

[a] Dr. G. Angulo
Institute of Physical Chemistry, Polish Academy of Sciences
Kasprzaka 44/52, 01-224 Warsaw (Poland)
Faxr: (+48) 22 632 3333
.
E-mail: gangulo@ichf.edu.pl
gonzalo_m_angulo@yahoo.es

[b] Dr. D. R. Kattnig, Dr. A. Rosspeintner, Prof. G. Grampp
Institute of Physical and Theoretical Chemistry
Graz University of Technology
Technikerstrasse 4/I, 8010 Graz (Austria)

[c] Prof. E. Vauthey
Department of Physical Chemistry, University of Geneva
30 quai Ernest-Ansermet, 1211 Geneva 4 (Switzerland)

Supporting information for this article is available on the WWW under http://dx.doi.org/10.1002/chem.200901693.

Only recently we used a diffusion-reaction theory, the "encounter theory",[1] which allows for a joint description of any kind of reaction and the influence of diffusion, regardless of the characteristics of the elementary reaction event, such as its distance dependence.[20] Making use of the differential version of the encounter theory we showed in a preceding paper[21] that the subtle details of the solvent structure and the hydrodynamic effect on the diffusion coefficient were needed to describe coherently the fluorescence decays on the nanosecond timescale and the steady-state quenching experiments in a wide range of viscosities and quencher concentrations. The importance of these two effects was first pointed out by Fayer et al.[8] In reference [22] we expanded our studies to the influence of the electron-transfer driving force, and were able to give a reasonable explanation for the so-called Rehm–Weller (RW) plateau.[19] Unfortunately, the two electron-transfer parameter sets obtained in references [21, 22] are not the same. Besides that, even the reaction rate models were not identical. Moreover, some additional problems with the stationary rate constant (obtained from the fluorescence decay traces after the diffusion regime had become stationary) remained unsolved: we found a concentration dependence for this rate constant similar in trend at all viscosities studied, but this quantity must, by definition, be independent of concentration!

In order to obtain full compatibility and comparability with the results obtained in our two previous publications,[21,22] we have employed the same fluorophore/quencher pair [bis(dimethylamino)-1,3-benzenedicarbonitrile (DMBCN)/1,3-dimethyl-2-nitrobenzene (MX2N)], as well as the solvent mixtures as used in reference [21]. Additionally, the fluorophore/quencher pair had also been included in our study on the free-energy dependence of fluorescence quenching.[22] In the present study, we have performed time-resolved experiments on the femto- to picosecond timescales by means of fluorescence up-conversion, with the aim of gaining insight into the static quenching and nonstationary quenching regimes. As explained above, this should, ideally, allow access to the diffusionless quenching reaction, thus enabling us to extract directly the electron-transfer parameters. We will relate the present findings to those presented in our two previous reports. Eventually, by re-evaluating some of our previous results, we will obtain a fully coherent picture of the non-Markovian quenching kinetics on time, concentration, driving force, and viscosity scales.

Theoretical Description and Approximations

With respect to our previous work,[21] we will introduce three modifications concerning the analysis of the data in order to explain the three sets of data simultaneously (the Stern–Volmer (SV) plots, the long-time asymptotes or nanosecond-resolved single-photon counting data (SPC), and the initial static and nonstationary quenching or picosecond-resolved fluorescence up-conversion data (FU)).

Firstly, a more comprehensive electron-transfer model, accounting for the solvent dielectric relaxation time and transitions to vibronically excited successor states, is utilized.[12,13,23,24] This is necessary because the fast transients can only be rationalized by fast initial electron-transfer rates, for which both effects become relevant. The same electron-transfer model has also been used in our analysis of the RW experiment; the model is shown in Equation (1) and the Levich–Dogonadze pre-exponential term is given by Equation (2).[22]

$$w(r) = \sum_{n=0}^{\infty} \frac{U(r)e^{-S}S^n}{n! + \tau_S U(r)e^{-S}S^n} \exp\left(-\frac{(\Delta G_I(r) + \lambda(r) + \hbar\omega n)}{4k_B T\lambda(r)}\right) \quad (1)$$

$$U(r) = \frac{V^2(r)}{\hbar}\sqrt{\frac{\pi}{k_B T\lambda(r)}} \quad (2)$$

In Equation (2), $V(r)$ stands for the diabatic matrix coupling element which is distance dependent and is defined in Equation (3), in which σ is the contact distance and L the decay of the coupling (equal to $2/\beta$ in other formulations[23]).

$$V(r) = V_\sigma \exp\left(-\frac{r-\sigma}{L}\right) \quad (3)$$

For the reorganization energy, we have either used Matsuda's empirical expression [Eq. (4)][25] (in which r_λ is a variable parameter accounting for the fact that generally the reorganisation energies at contact are found to be overestimated by the Marcus expression), or alternatively the more common and physically better grounded expression given in Equation (5),[26] valid for reactants of equal size, which constitutes a good approximation in our case.

$$\lambda(r) = \lambda(\infty) - \frac{r_\lambda k_B T}{r} \quad (4)$$

$$\lambda(r) = \lambda(\sigma)\left(2 - \frac{\sigma}{r}\right) \quad (5)$$

The Marcus reorganization energy expressions for infinite, $\lambda(\infty)$, and close-contact separation, $\lambda(\sigma)$, obey Equation (6), in which n stands for the refractive index of the solvent, and ε_S for its static dielectric constant.

$$\lambda(\infty) = 2\lambda(\sigma) = \frac{e_0^2}{2\pi\varepsilon_0\sigma}\left(\frac{1}{n^2} - \frac{1}{\varepsilon_S}\right) \quad (6)$$

The great advantage of the solvent mixtures used is that the reorganization energy is kept constant, whereas the viscosity is adjustable over a very wide range by adding increasing amounts of glycerol to dimethylsulfoxide (DMSO).

The distance dependence of the Gibbs free energy is expressed by the Weller equation, shown in Equation (7), in which E_{ox} and E_{red} are the standard potentials of oxidation and reduction for the donor and the acceptor in electron volts, respectively, E_{00} is the excited state energy of the fluo-

rophore, and r_c is the Onsager radius, which here varies only slightly with the solvent composition used.[27]

$$\Delta G_I = E_{ox}(D^+/D) - E_{red}(A/A^-) - E_{00} - k_B T\frac{r_c}{r} \quad (7)$$

The model assumes that the dielectric response of the solvent obeys Debye's law with a single relaxation time, τ_D. The solvent relaxation time in Equation (1) relates to the longitudinal relaxation time ($\tau_L = \tau_D \varepsilon_\infty/\varepsilon_S$, with ε_∞ being the dielectric constant of the medium at infinite electrical field frequency which is also approximated to be constant in the solvent mixtures used, vide infra) as shown in Equation (8).

$$\tau_S = 4\tau_L\sqrt{\frac{\pi k_B T}{\lambda(r)}} \quad (8)$$

The multichannel parameters are the Huang–Rhys factor $S = \lambda_q/\hbar\omega$, which stands for the strength of the coupling between the single reactant mode and the n^{th} vibronic product mode, and depends on the inner reorganization energy (λ_q) associated with the effective vibrational mode of frequency (ω).

Equation (1) represents an interpolation between the perturbative electron-transfer regime, applicable for small coupling matrix elements, and the Zusman expression for solvent-controlled electron transfer in the high friction limit. This interpolation is carried out individually for every vibronic transition. The validity is therefore limited by the requirement that the effective coupling matrix element, $V_{eff}(r) = V(r)\sqrt{\exp(S)S^n/n!}$, must not exceed $k_B T$.[28] Beyond this limit, the barrier region is more parabolic than cusp, and Kramers' expression for solvent-controlled electron transfer[29] is more applicable. Furthermore, the reduction of the barrier height by the strong coupling is then no longer negligible. Equation (1) has also been successfully applied to the forward electron transfer in the perylene/tetracyanoethylene system.[12,13] Matsuda et al. applied a similar, though not identical, model in their analysis of the RW plot.[25]

Secondly, the change of the viscosity with the quencher concentration has been explicitly accounted for. In our previous study, this effect had been disregarded, since it usually did not exceed 3% (at most 8.4% for $\eta = 32$ cP at a quencher concentration of 0.5 M).

Finally, a phenomenological correction yielding an effective acceptor concentration has been introduced in order to account for the reduction of the stationary quenching rate constant (k_∞) with the formal quencher concentration (c_f). To this end we postulate that the ideal stationary rate constant at a given viscosity ($k^i_\infty(\eta)$), does not (except for its response to viscosity) depend on the quencher concentration. The observed reduction in k_∞ is then tantamount to a reduction in the actual quencher concentration (c_a), or in other words, to the activity coefficient of the quencher. We deliberately do not specify the reason for the reduction in k_∞. The reader is referred to the Supporting Information accompanying this article for details.

Differential encounter theory (DET) has been employed in the same manner as we have presented it before. We just summarize it here, and the interested reader can find more detailed descriptions in references [1,21,22,30]. The excited-state population decay follows the kinetic expression given in Equation (9).

$$\frac{dN_F(t)}{dt} = -\left(k(t)c + \tau_F^{-1}\right)N_F(t) \quad (9)$$

Equation (9) has the solution shown in Equation (10), in which the rate constant for the ionization (quenching) reaction is defined as in Equation (11).

$$N_F(t) = N_F(0)\exp\left(-\frac{t}{t_F} - c\int_{t'=0}^{t} k(t')dt'\right) \quad (10)$$

$$k(t) = \int_V w(r)n(r,t)dV \quad (11)$$

In Equation (11), $n(r,t)$ is the reactant pair distribution function, which is the solution of the auxiliary diffusion-reaction equation [Eq. (12)], solved with the boundary conditions given in references [21,22].

$$\frac{\partial n(r,t)}{\partial t} = \hat{L}(r)n(r,t) - w(r)n(r,t) \quad (12)$$

The diffusion operator, $\hat{L}(r)$, obeys Equation (13).

$$\hat{L}(r) = \frac{1}{r^2}\frac{\partial}{\partial r}D(r)r^2\exp(-v(r))\frac{\partial}{\partial r}\exp(+v(r)) \quad (13)$$

The diffusion coefficient is either expressed by the Deutch–Felderhof expression [Eq. (14)] or by the Northrup–Hynes expression [Eq. (15)], and $v(r) = -\ln(r)$ in which $g(r)$ is the solvent structure as obtained from the solution of the Percus–Yevick equation.[31]

$$D(r) = D_\infty\left(1 - \frac{3\sigma}{4r}\right) \quad (14)$$

$$D(r) = D_\infty\left(1 - \frac{1}{2}\exp\left(-\frac{r-\sigma}{\sigma}\right)\right) \quad (15)$$

The steady-state quenching rate constant, $\kappa(c)$, obtained from the steady-state experiments, is defined by the SV expression [Eq. (16)], in which I is the fluorescence intensity in the presence of a quencher of concentration c, and I_0 is the fluorescence intensity in the absence of a quencher.

$$\frac{I}{I_0}=\frac{\int_0^\infty N(c,t)\mathrm{d}t}{\int_0^\infty N(0,t)\mathrm{d}t}=\frac{1}{\tau_F}\int_0^\infty \exp\left(-\frac{1}{\tau_F}-c\int_0^t k(t')\mathrm{d}t'\right)\mathrm{d}t=\frac{1}{1+c\tau_F\kappa(c)} \quad (16)$$

On the other hand, the stationary quenching rate constant is given by Equation (17).

$$k_\infty=4\pi\int_\sigma^\infty r^2 w(r)n_S(r)\mathrm{d}r \quad (17)$$

It is customary to cast k_∞ in a form equivalent to the Smoluchowski expression for the diffusion rate constant [Eq. (18)].

$$\lim_{t\to\infty}k(t)=4\pi R_Q D \quad (18)$$

Note, however, that the effective quenching radius, R_Q, does usually exceed the contact radius, σ. It can be obtained from the SPC experiments as described in reference [21].

Results and Discussion

Following the same strategy as in the previous paper, we have fitted the reaction-diffusion model described above to the SV plots [Eq. (16)] (for a schematic description of the procedure see Scheme SI.1 in the Supporting Information). In particular, the coupling matrix element (V_σ) and its decay length (L) have been adjusted. For a total of eight solvent mixtures, with viscosities ranging from 2.2 to 62 cP, the diffusion coefficient was modeled as shown in Equation (19), in which the subscript refers to the composition of the solvent, and $\eta(c)$ denotes the dynamic viscosity of the solution after adding the liquid quencher, MX2N. The d_is have been adjusted freely. Note that a value of $d_i=133$ or 200 $Å^2ns^{-1}cP$ is expected for $r_F=r_Q=\sigma/2=3.25$ Å based on the Stokes–Einstein relation with stick or slip boundary conditions, respectively.

$$D_i(c)=\frac{d_i}{\eta(c)} \quad (19)$$

Using the input parameters in Table 1, the parameters compiled in Table 2 yield a satisfactory description of the SV plots (the parameters used to account for the electron-transfer reaction and the diffusive motion of the reactants have been scrutinized in references [21,22]) for all eight combinations (I–VIII) of models for the reorganization energy, the diffusion coefficient, and the solvent structure. Concerning the multichannel ET parameters, we have used the same values as for the analysis of the Rehm–Weller plot (see reference [22] for a detailed discussion). For all combinations in which the solvent structure and the hydrodynamic effect have been simultaneously accounted, a decay length of $L\approx2$ Å has been found. This value is of similar size to those found previously for the reactions between perylene and *N*,*N*-dimethylaniline or rubrene and duroquinone, for example.[32,33] Note that McLendon et al.[34] have determined a coupling decay constant of 1.4 Å for glassy glycerol matrices. This is not in disagreement with this work, as one might

Table 1. Properties of the system and input parameters for the electron-transfer reaction (ETR).

DMBCN	$\tau_F=22.4$ ns $\phi_F=0.55$ $E_{00}=2.72$ eV E_{ox} (vs. SCE) $=0.73$ V
MX2N	E_{red} (vs. SCE) $=-1.40$ V
DMSO-GLY	$n=1.48$ $\varepsilon_S=48$ $\lambda_{MARCUS}(\sigma)=0.97$ eV $r_c=11.9$ Å $\tau_L=0.8$ ps
ETR input parameters	$\sigma=6.5$ Å $\Delta G(\sigma)=-0.63$ eV $\lambda_q=0.42$ eV $\omega=0.186$ eV $T=293.15$ K

Table 2. Fitting parameters obtained by analyzing the SV plots using combinations of different models for the reorganization energy and the hydrodynamic hindrance, and by making optional allowance for the solvent structure. DF and NH denote the hydrodynamic friction models according to Deutch and Felderhof [Eq.(14)] and Northrup and Hynes [Eq.(15)], respectively. The row labeled $g(r)$ indicates whether the solvent structure has been accounted for. Combinations that do not take the latter into account are incompatible with the fast initial decay detected by the FU technique. For $\lambda(\sigma)/\lambda_{MARCUS}(\sigma)=0.62$ the empirical model in Equation (4) has been used to evaluate the reorganization energy. The d_i parameters are given in units of $Å^2ns^{-1}cP$. $\sigma=6.5$ Å and $T=293$ K. r_{SV} gives the root mean square relative errors for the concentration-dependent SV constant, $\kappa(c)$. All fits of the SV plots are visually indistinguishable. A differentiation of different parameter sets is possible by considering the agreement of the simulations with the long-time quenching rate constant, expressed here in terms of the quenching radius, R_Q. For the latter, r_{TR} gives the root mean square residual norm observed for the 8 datasets.

	I	II	III	IV	V	VI	VII	VIII
$g(r)$	YES	YES	YES	YES	YES	YES	NO	NO
D	DF	DF	NH	NH	–	–	DF	DF
$\lambda(\sigma)/\lambda_{MARCUS}(\sigma)$	1	0.62	1	0.62	1	0.62	1	0.62
V_σ [meV]	50	22	49	18	30	13	55	29
L [Å]	2.0	1.9	2.0	2.0	2.4	2.3	2.1	1.8
d_1 [62 cP]	118	146	96	113	75	95	105	141
d_2 [32 cP]	136	157	109	123	90	104	120	147
d_3 [18 cP]	127	139	100	108	84	91	112	126
d_4 [12 cP]	129	138	102	108	85	91	113	124
d_5 [8.0 cP]	121	126	94	98	79	82	105	112
d_6 [5.2 cP]	120	121	92	94	77	79	104	106
d_7 [3.3 cP]	106	106	82	82	69	69	92	93
d_8 [2.2 cP]	88	86	67	67	58	55	77	74
r_{SV} [%]	0.46	0.49	0.48	0.50	0.50	0.52	0.48	0.50
r_{TR} [Å]	0.20[a]	0.18[a]	0.25[a]	0.24[a]	0.45[a]	0.37[a]	0.30[a]	0.41[b]

[a] Systematic positive deviation of the experimental points. [b] Systematic negative deviation of the experimental points.

be tempted to assume at first glance: the value predicted for the coupling decay depends on the overall distance dependence of the electron-transfer model, and not just on the intrinsic dependence of coupling on distance. In the Marcus normal region, the distance dependence of the reaction probability can indeed be well approximated by the exponential model. However, in doing so, a smaller effective value of L is to be expected compared to that resulting from the full-fledged Marcus ET model.[9] Since McLendon's value is based on the exponential model, it is not in conflict with our data. Indeed, a value close to or larger than $L=2$ Å was obtained when a more comprehensive ET model was employed (the exact value again depends on the overall r dependence).

The Marcus expression for the reorganization energy [Eq. (5)] gives rise to a larger V_σ than Matsuda's proposal [Eq. (4)], which has been utilized here with $r_\lambda k_B T = 8.7$ Å eV. This is not surprising in view of the fact that for the latter the reorganization energy at contact amounts to only 62% of the Marcus value ($\lambda(\sigma)=0.60$ vs. 0.97 eV). In fact, combination II results in the best agreement for the quenching radii, R_Q. However, due to its empirical nature, we did not pursue this reorganization energy model any further. Therefore, only combination I, which is superior to combinations III–VIII in explaining the changes of quenching radii with viscosity, will be discussed in the following sections. This combination yields $L=2.0$ Å and $V_\sigma=50$ meV. These parameter values agree strikingly with those obtained previously in our study on the RW experiment[22] (although with a larger $\lambda(\sigma)$). Figure 1 allows a comparison of simulated and experimental quenching rate constants, $\kappa(c)$.

A multitude of parameter sets yield quasi-identical fits for the SV plot. A differentiation of these sets is, however, possible by considering the long-time limit of the diffusion-influenced quenching rate constant [Eqs. (17) and (18)], which we express in terms of the quenching radius, R_Q, in Equation (20), in which $D(\eta)$ is the bulk diffusion coefficient (see the Supporting Information for more details about $k^i_\infty(\eta)$).

$$R_Q = \frac{k^i_\infty(\eta)}{4\pi D(\eta)} \tag{20}$$

Based on the parameter set I given above, the dependence of R_Q on D given in Figure 2 is obtained. Except for the point corresponding to the second highest viscosity, all experimental quenching radii exceed the simulated results, the deviation being typically smaller than 10%. Nonetheless, the trend followed by the experimental points clearly obeys that given by the simulations. In fact, the deviation of R_Q as given in Figure 2 is systematic, and discerning its cause is not difficult: In determining the R_Q values from the single-photon-counting traces, we made use of the long-time Smoluchowski asymptote [Eq. (21)],[1,35] together with Equation (20) and the diffusion coefficients obtained from the analysis of the SV plots.[36]

$$k_{Smolu}(t) = k_\infty\left(1+\frac{k_\infty}{4\pi D}\frac{1}{\sqrt{\pi D t}}\right) \tag{21}$$

Equation (21) is expected to hold for times significantly exceeding $R_Q^2/D \geq \tau_{Diff} = \sigma^2/D$.[1,9] However, given the finite number of sampled decay events in combination with a non-zero number of dark counts, the single-photon-counting curves contain kinetic information only up to a certain time; the faster the quenching and the smaller the excited-state lifetime of the fluorophore, the shorter the time. In order to have a significant portion of the decay curve avail-

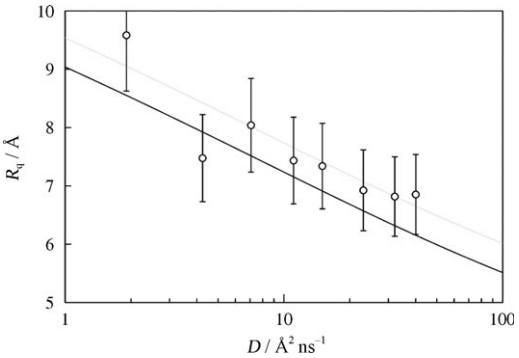

Figure 2. Dependence of the quenching radius, R_Q, on the diffusity, D. The bullets give the experimental values as extracted from the asymptotes of $k_\infty(c_F\eta)$ in the $c\rightarrow 0$ limit. The diffusion coefficients predicted by the analysis of the SV experiments have been used. The solid line reproduces the simulation using parameter set I as given in Table 2. The quenching radius of a purely diffusion-controlled contact reaction amounts to only 4.0 Å under the same conditions (due to the hydrodynamic hindrance and the small contact radius). This effective radius is evaluated from $\sigma_{eff}^{-1} = D\int D(r)^{-1}e^{v(r)}r^{-2}dr$.[21] The reaction analyzed here is, thus, clearly identified as a distant quenching reaction. The gray dotted line corresponds to the simulation shifted by +0.5 Å. It has been added to underline the correct trend of the simulation. An error of 10% has been arbitrarily assumed.

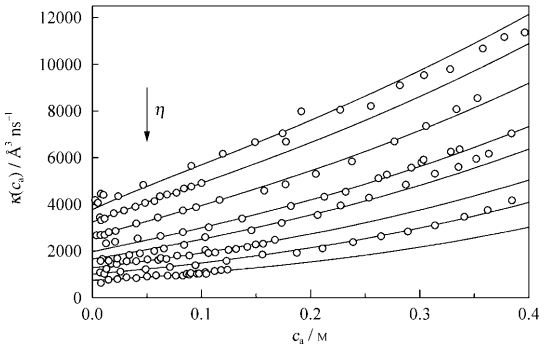

Figure 1. Anamorphosis of the conventional SV plot, allowing for a better appreciation of the dependence of $\kappa(c)$ on concentration and viscosity. All available datasets are shown. The solid lines reproduce the fits for combination I, which is based on Marcus' multi-channel electron-transfer model [Eq. (1)], Deutch–Felderhof hydrodynamic hindrance [Eq. (14)], and solvent structures obtained from Monte Carlo simulations (for a quencher concentration of 0–0.5 M).[21] The fit parameters are available in Table 2.

able for analysis, we were thus forced to commence the fitting by Equation (21) at $t=\tau_{Diff}$. At this instance of time, however, the (true) time-dependent rate constant evaluated by DET, $k(t)$, exceeds its approximation given by Equation (21) [with R_Q evaluated from Eq. (17)] significantly. As a consequence, the experimental R_Q values systematically exceed the true ones. It has to be noted that the stationary limit is not actually attained here within the time window of the SPC experiments. This holds true even though a fluorophore with a long excited-state lifetime has been employed. The discrepancy is expected to be even more stringent for studies using fluorophores with fluorescence lifetimes of several nanoseconds only. The latter are in fact not rare in the scientific literature.[37] A proof of this claim is available in Figure 3, which reproduces the ratio of $k(t)/k_{Smolu}(t)$ as a

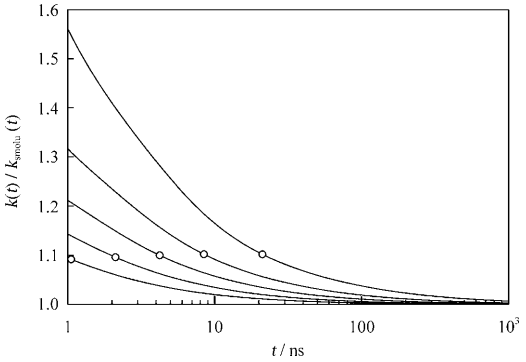

Figure 3. Ratio of the time-dependent quenching rate coefficient, $k(t)$, and its long-time approximation as evaluated from Equation (21) with the pertinent R_Q determined from the steady state distribution of $n_S(r,t)$. The same parameters as for Figure 1 have been used. For each curve τ_{Diff} is marked by a circle.

function of time for several diffusion coefficients. Note that for the experimentally accessible part of the decay curve, $k(t)>k_{Smolu}(t)$ by approximately 10%. Furthermore, the deviation from the Smoluchowski limit is expected to increase with increasing quencher concentration, because the experimentally accessible time window is shortened by the quenching process. We have tested whether this gives rise to an additional concentration dependence of $k_\infty(\eta)$. It turns out that for the measurements conducted here, the effect is negligible; that is, for decays spanning at least 50 ns, the additional variation of R_Q due to different concentrations within a series amounts to less than 1%. All $k_\infty(\eta)$ and thus all R_Q values of the entire series are, however, systematically shifted to larger values, with the effect being more pronounced in viscous solvents. Moreover, the stationary rate constants extracted from the long-time asymptotes are weakly correlated with the diffusion coefficient assumed for its determination by Equation (21). In Figure 2 we utilize the $k^i_\infty(\eta)$ that are appropriate for the diffusion coefficient as determined from the SV plots through Equation (19). Empirically, a linear dependence of $k^i_\infty(\eta)$ on the D used for its determination has been found (not shown).

The virtue of our novel approach is that the short-time quenching, which was not compliant with the electron-transfer model used in reference [22], can now be accounted for. We have two sets of FU measurements available that reveal the early events closely related to the static quenching. For one set, a fixed concentration of MX2N (0.34 M) has been used, and the fluorescence decay has been recorded at five different viscosities with a sampling interval of 3 ps. The second set pertains to the quenching in DMSO, which has been comprehensively discerned at four different concentrations, ranging from 0.2 to 0.5 M, with points every 0.1 ps.

With the very same set of parameters as used above (combination I) the initial fluorescence decays at the different viscosities can be simulated (set I). Only the shift of the first point with respect to the delta excitation response function and its relative amplitude have to be introduced as adjustable parameters. The time-shift has been uniformly set to 4 ps, a value suggested by comparing the kinetic term [Eq. (22)] with that of the experiments from the second set, which exhibit a higher point density at short times.

$$\int_0^t k(t')\mathrm{d}t' = -(\ln(I/I_0) + t/\tau_F)/c \qquad (22)$$

Indeed, within the time frame available for the different experiments, we found matching kinetic terms. This suggests that the assumption of one dielectric relaxation time independent of solvent composition is in fact appropriate. Figure 4 gives the analysis of the initial fluorescence decay, with the relative amplitude of the first point being the only free parameter. For all curves, a value of 0.8 for the latter gave the best agreement. The diffusion coefficient of the mixtures was determined by interpolating the d_i values from the SV fit with respect to the mole fraction of glycerol. Given that the electron-transfer parameters have, in essence, been determined from the SV plots and not further re-adjusted, this is a good agreement of theory and experiment. Note, also, that no second decay channel, which has been frequently invoked for similar studies, is necessary to account for the data. In addition, no increase in the coupling matrix element (V_σ) is required.

Finally, the short-time quenching in DMSO at different concentrations shall be addressed. Figure 5 reproduces the experimental decays together with the simulations. No adjustable parameter has been used at all. The diffusion coefficient was determined from the appropriate d_i. The agreement is apparently good, but abates with increasing quencher concentration. Note, however, that the larger effective concentrations even exceed those utilized in the SV plot. Our attempts to improve the fits have thus far always resulted in suboptimal SV simulations. The contribution of a second (contact) reaction channel, contributing mainly to the static quenching process at the highest quencher concentrations used here, is possible, although clearly not overwhelming.

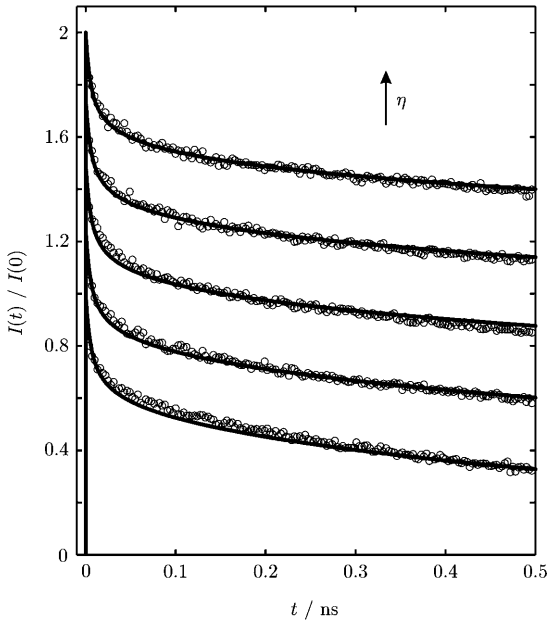

Figure 4. Initial fluorescence decay for the quenching of DMBCN by MX2N in DMSO/glycerol mixtures of varying viscosities, recorded at a time increment of 3 ps. Experimental points are represented by circles, and fits by solid lines. From bottom to top the concentrations of the quencher are $c=0.34$, 0.35, 0.35, 0.34, and 0.34 M, and the solvent viscosities are $\eta=3.8$, 6.7, 11, 15, and 20 cP. The diffusion coefficients have been evaluated from $D_i=d_i/\eta(c)$, determining the pertinent d_i by cubic interpolation from the results of the SV analysis. The effect of dilution by the quencher has been accounted for. As expected, the effects originating from diffusion and the fluorescence decay (τ_F) are small during the first 0.5 ns. The electron-transfer parameters have been taken from Table 2, dataset I. The relative amplitude of the initial point is the only adjustable parameter. For the least-square fit illustrated here it takes the value of 0.8.

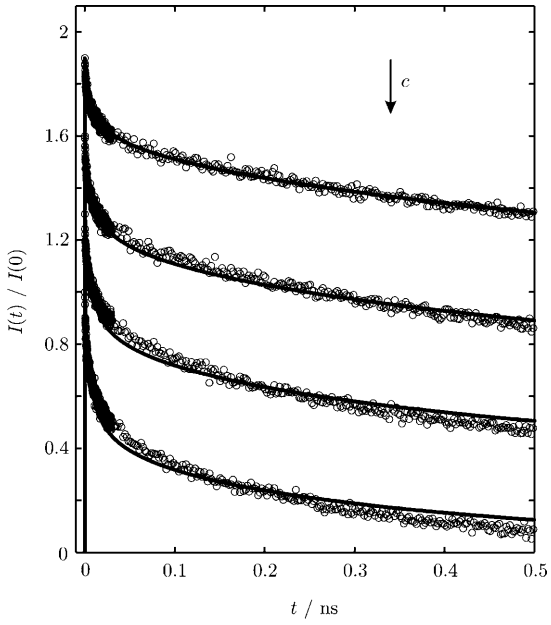

Figure 5. Initial fluorescence decay for the quenching of DMBCN by different (high) concentrations of MX2N in DMSO ($\eta=2.2$ cP) recorded with a time increment of 0.1 ps. The effective concentrations from bottom to top are 0.51, 0.38, 0.30, and 0.22 M. The electron-transfer parameters compiled for combination I have been used, without any adjustable quantity. Simulations are represented by solid lines.

Conclusion

We have successfully explained the fluorescence deactivation of DMBCN by MX2N in a variety of solvent systems exhibiting moderate to high viscosities. Our approach builds on a remote electron-transfer model, which accounts for the solvent dielectric relaxation time and the transfer to vibronically excited successor states. By accounting fully for the solvent structure and the hydrodynamic effect, a coherent description of time-resolved and steady-state experiments has been achieved. On the other hand, no consistent description of all the data is possible without including all these features simultaneously. Once the appropriate model has been chosen, the analysis of the steady state deactivation for at least ten concentrations in the bending region of the SV plot is sufficient to determine the pertinent electron-transfer parameters.

However, discerning the suitability of different electron-transfer models is ultimately only possible by detecting the initial static and non-stationary decay. The appropriate choice of contact distance is critical, that is, by choosing larger smaller ones the steady-state quenching data as well as the long-time asymptotes may often be described in terms of a diabatic or an adiabatic electron-transfer model. It is important to note that in the present case, the chosen contact distance leads to values for the coupling matrix element and its corresponding decay length, which are within the applicability and physical meaningful limits of the electron-transfer model used. This would not be the case for other radii.

Here, the entire quenching process, comprising the fast, static initial decay, the beginning non-stationary transients, the long-time asymptote, and the integral fluorescence, has been comprehensively described without requiring the inclusion of a second fast contact or remote (decay to excited ions) deactivation channel, which are frequently postulated in similar studies. It is quite likely that the inclusion of many of these additional reaction channels could be avoided by taking the discrete nature of the solvent (the solvent structure) into account. The latter is unquestionably present for any solvent (unlike a second decay channel), and failure to take it into account may lead one to unnecessarily postulate artificial reaction channels. It is our conviction that many previous publications ought to be revisited by properly accounting for the details of diffusive motion, the solvent structure, and hydrodynamic hindrance.

The fast initial fluorescence deactivation is often attributed to so-called tight ion pairs (TIP). Although its direct spectroscopic observation has not been realized until recently,[38] the TIP has always been regarded as a transient contact species, which is distinguished from the solvent-separated ion pair (SIP) by an exceptionally large electronic coupling and, thus, a fast intrinsic ET reaction rate, irrespective

of the free energy difference. Arguably, the notion of the TIP hence belongs to the realm of exciplex formation rather than that of outer-sphere ET. The data presented here do not indicate a significant contribution attributable to the TIP up to a quencher concentration of at least 0.3 M. In particular, the fluorescence deactivation can be fully explained in terms of a single ET process with distance-dependent reactivity, which in the TIP/SIP model would rather be attributed to the SIP.[39] Some caution might be appropriate here. The model used here is based on the use of the Marcus expression for reorganization energy, which is fine for large distances and large reactants, but probably not at close distances. The reactants are also supposed to be spheres with an exponential dependence of V with distance. In this case the nature of a SIP is quite clear, because distance is the only parameter that controls V and λ. However, real systems are not like this. SIP is clearly a pair where the ions are less coupled, but there are other degrees of freedom than just distance. Thus, the transformation of the distance obtained from the model into a molecular parameter is perhaps not so evident.

To the knowledge of the authors this is the first time that such a comprehensive set of data (comprising ultrafast to nanosecond time-resolved decays, steady-state fluorescence quenching, viscosity change, and concentration change) has been quantitatively described by means of a physically grounded bimolecular electron-transfer model. Moreover, the final set of parameters found for the electron-transfer elementary reaction are compatible with the driving-force dependence of the quenching rate constant for the same fluorophore.

Experimental Section

Chemicals: The synthesis and properties, mainly photophysical, of the fluorophore, 2,5-bis(dimethylamino)-1,3-benzenedicarbonitrile (DMBCN), have been described elsewhere.[40] The sources of the quencher, 1,3-dimethyl-2-nitrobenzene (MX2N), and of the solvents and their handling, were the same as in references [21,22]. Table 1 details the relevant properties of the system.

Procedures and apparatuses: The fluorescence up-conversion (FU) measurements were performed by means of a home-built setup. The laser source was a Kerr lens mode-locked Ti:Saphire oscillator (KMLabs) delivering about 30 fs pulses around 800 nm at a repetition rate of 40 MHz and a power of about 400 mW, pumped by 5.2 W at 527 nm of a Nd:YVO4 laser (Millenia VIs Spectra Physics). The output pulses were pre-compressed before being frequency doubled in a BIBO crystal, and the resulting 400 nm pulses were focused into the rotating cell containing the sample (of typically 0.4 mm thickness), whereas the remaining 800 nm pulses were deferred by a motorized delay line. The fluorescence was then mixed with the 800 nm gating pulses in another BIBO crystal for up-conversion. The resulting UV output was focused into a Cornerstone 260 1/4 m monochromator equipped with a photomultiplier tube (R654P Hamamatsu) operating in the photon-counting mode. Instead of transmissive elements (except for a 400 nm dielectric mirror to separate the 800 and 400 nm beams, a half-wave plate to control the 400 nm polarization, a 2 A Kodak Wratten Gelatin filter of 0.1 mm to remove the 400 nm remaining excitation beam after the sample, and a dichroic mirror to bring the gating pulses to the second nonlinear crystal at an angle of 10° with the fluorescence), off-axis parabolic mirrors were used to focus and to collimate both the gating and the pump beams as well as the fluorescence. Under these conditions, a Gaussian instrument response function of 70 fs FWHM could be obtained. The experiment was computer-controlled using a Labview-based program.

DMBCN fluorescence was monitored at 520 nm, a wavelength at which the measured time profiles are not affected by the solvation-induced dynamic Stokes shift in DMSO. All measurements were performed under magic angle conditions to avoid anisotropy effects.

The quencher concentration was adjusted to approximately 0.3 M for the viscosity-dependence measurements, and between 0.2 and 0.5 M for the concentration dependence in DMSO. See the Supporting Information for the fine determination of these concentrations.

The other experiments mentioned in this paper were as described in references [21,22].

Acknowledgements

G.A. would like to thank Dr. Anatolio Pigliucci for his work on the fluorescence up-conversion setup described here, as well as Dominique Lovy from the University of Geneva for his valuable help with the same setup. This work has been performed thanks to the financial support of the University of Geneva. A.R. and D.R.K. would like to thank Lola Rodríguez Hidalgo and Jakob Grilj, respectively, for their hospitality during their short stay in Geneva.

[1] A. I. Burshtein, *Adv. Chem. Phys.* **2000**, *114*, 419–587; A. I. Burshtein, *Adv. Chem. Phys.* **2004**, *129*, 105–418.
[2] B. Paulson, K. Pramod, P. Eaton, G. Closs, J. R. Miller, *J. Phys. Chem.* **1993**, *97*, 13042–13045.
[3] J. W. Verhoeven, *J. Photochem. Photobiol. C* **2006**, *7*, 40–60.
[4] B. Albinsson, J. Mårtensson, *J. Photochem. Photobiol. C* **2008**, *9*, 138–155.
[5] A. Ponce, H. B. Gray, J. R. Winkler, *J. Am. Chem. Soc.* **2000**, *122*, 8187–8191.
[6] H. B. Gray, J. R. Winkler, *Proc. Natl. Acad. Sci. USA* **2005**, *102*, 3534–3539.
[7] D. E. Eads, B. G. Dismer, G. R. Fleming, *J. Chem. Phys.* **1990**, *93*, 1136–1198.
[8] S. F. Swallen, K. Weidemaier, H. L. Tavernier, M. D. Fayer, *J. Phys. Chem.* **1996**, *100*, 8106–8117.
[9] V. S. Gladkikh, A. I. Burshtein, H. L. Tavernier, M. D. Fayer, *J. Phys. Chem. A* **2002**, *106*, 6982–6990.
[10] N. Mataga, H. Miyasaka, *Prog. React. Kinet.* **1994**, *32*, 317–430.
[11] L. Burel, M. Mostafavi, S. Murata, M. Tachiya, *J. Phys. Chem. A* **1999**, *103*, 5882–5888.
[12] V. Gladkikh, A. I. Burshtein, G. Angulo, S. Pages, B. Lang, E. Vauthey, *J. Phys. Chem. A* **2004**, *108*, 6667–6678.
[13] V. Gladkikh, A. I. Burshtein, S. V. Feskov, A. I. Ivanov, E. Vauthey, *J. Chem. Phys.* **2005**, *123*, 244510/1–11.
[14] H. L. Tavernier, M. M. Kalashnikov, and M. D. Fayer, *J. Chem. Phys.* **2000**, *113*, 10191–10201.
[15] M. Tachiya, S. Murata, *J. Am. Chem. Soc.* **1994**, *116*, 2434–2436.
[16] C. Turró, J. M. Zaleski, Y. M. Karabatsos, D. G. Nocera, *J. Am. Chem. Soc.* **1996**, *118*, 6060–6067.
[17] G. L. Hug, B. Marciniak, *J. Phys. Chem.* **1995**, *99*, 1478–1483.
[18] M. Tachiya, S. Murata, *J. Phys. Chem.* **1992**, *96*, 8441–8444.
[19] D. Rehm, A. Weller, *Isr. J. Chem.* **1970**, *10*, 259–271.
[20] A multitude of approaches addressing the diffusion influence of distance electron-transfer phenomena has been suggested. We employ the DET framework here, as it has proven valuable in a variety of related studies. However, we do not imply that DET is the only model able to comprehensively account for the experimental data. The inclined reader should realize that DET and the approach paved by Tachiya and Fayer are equivalent, with one resulting from

the other by adjoining the differential operator of the diffusion equation. The mathematical tools necessary to prove the equivalence of these and related Sturm–Liouville problems are, for example, summarized in *Mathematics for Physicists* (Eds.: P. Dennery, A. Krzywicki), Dover, New York.

[21] A. Rosspeintner, D. R. Kattnig, G. Angulo, S. Landgraf, G. Grampp, A. Cuetos, *Chem. Eur. J.* **2007**, *13*, 6474–6483.

[22] A. Rosspeintner, D. R. Kattnig, G. Angulo, S. Landgraf, G. Grampp, *Chem. Eur. J.* **2008**, *14*, 6213–6221.

[23] A. Barzykin, P. Frantsuzov, K. Seki, M. Tachiya, *Adv. Chem. Phys.* **2002**, *123*, 511–616.

[24] L. Zusman, *Chem. Phys.* **1980**, *49*, 295–304.

[25] N. Matsuda, T. Kakitani, T. Denda, N. Mataga, *Chem. Phys.* **1995**, *190*, 83–95.

[26] R. A. Marcus, *J. Chem. Phys.* **1956**, *24*, 979–989; R. A. Marcus, *J. Chem. Phys.* **1957**, *26*, 867–871.

[27] A. Weller, *Z. Phys. Chem.* **1982**, *130*, 129–138.

[28] V. Gladkikh, A. I. Burshtein, I. Rips, *J. Phys. Chem. A* **2005**, *109*, 4983–4988.

[29] H. A. Kramers, *Physica* **1940**, *7*, 284–308.

[30] D. Kattnig, Thesis, Institute of Physical and Theoretical Chemistry (Graz), **2008**.

[31] L. Tsang, J. A. Kong, K.-H. Ding, C. O. Ao, *Scattering of Electromagnetic Waves, Numerical Simulations*, 1st ed., Wiley-Interscience, New York, **2001**.

[32] A. Rosspeintner, G. Angulo, M. Weiglhofer, S. Landgraf, G. Grampp, *J. Photochem. Photobiol. A* **2006**, *183*, 225–235.

[33] S. F. Swallen, K. Weidemaier, M. D. J. Fayer, *Chem. Phys.* **1996**, *202–213*, 2976–2986.

[34] S. Strauch, G. McLendon, M. McGulre, T. Guarr, *J. Phys. Chem.* **1983**, *87*, 3579–3581.

[35] M. von Smoluchowski, *Z. Phys. Chem.* **1917**, *92*, 129–168.

[36] Due to the formal correspondence with Smoluchowski's influential expression for the probability of coagulation (with R_Q substituting σ) we will henceforth refer to Equation (21) as the Smoluchowski asymptote.[1,35] Note, however, that Equation (21) is generally valid, whereas Smoluchowski has assumed a black sphere.[1] Note furthermore that the k_∞ values extracted from the time traces are only marginally dependent on the particular choice of D, when chosen in the range preset by the stick and slip boundary condition. Thus, k_∞ needs to be extracted only once. Confer to ref. [21] for details on the data handling protocol. In general, the Smoluchowski asymptote is expected to hold for times significantly exceeding $R_Q^2/D \geq \tau_{Diff} = \sigma^2/D$.[1,9]

[37] V. Avila, C. M. Previtali, C. A. Chesta, *Photochem. Photobiol. Sci.* **2008**, *7*, 104–108.

[38] O. F. Mohammed, K. Adamczyk, N. Banerji, J. Dreyer, B. Lang, E. T. J. Nibbering, E. Vauthey *Angew. Chem.* **2008**, *120*, 9184; *Angew. Chem. Int. Ed.* **2008**, *47*, 9044 –9048.

[39] Note, however, that a priori differential encounter theory does not require a strict distinction of the SIP or TIP, the transition being (possibly) smooth. Indeed, the TIP could, in the DET picture, be introduced either as an "efficiently coupled" ion pair or as an additional contact species. Literature suggests the second proposition, which is also assumed here. It is crucial to note that a TIP-free model is sufficient for modeling the diffusive ET deactivation at low to moderate concentrations in most cases. This statement also applies to the interpretation of the Rehm-Weller experiment given in ref. [22]. Apparently, the effective reaction volume associated with the TIP is too small to contribute significantly, except possibly at exceptionally large concentrations. It is expected that the recent advancement in spectroscopic techniques will stimulate research on the bending questions of the TIP. Our study makes it clear that no correct interpretation of these experiments will be possible without due consideration of the solvent structure.

[40] G. Angulo, G. Grampp, A. A. Neufeld, A. I. Burshtein, *J. Phys. Chem. A* **2003**, *107*, 6913–6919..

Received: June 19, 2009
Revised: October 3, 2009
Published online: January 11, 2010

